DC-to-DC Efficiency Maximization in Wireless Power Transfer with PA and Rectifier Nonlinearities via Semidefinite Relaxation

Young-Seok Lee
Inst. New Media Commun.
Dept. of Electr. and Comput. Eng.
Seoul National University
Seoul, Republic of Korea
ryanlee@snu.ac.kr

Taeyeong Yoon
Inst. New Media Commun.
Dept. of Electr. and Comput. Eng.
Seoul National University
Seoul, Republic of Korea
taeyeong.yoon@snu.ac.kr

Sangwook Nam
Inst. New Media Commun.
Dept. of Electr. and Comput. Eng.
Seoul National University
Seoul, Republic of Korea
snam@snu.ac.kr

Jungsuek Oh
Inst. New Media Commun.
Dept. of Electr. and Comput. Eng.
Seoul National University
Seoul, Republic of Korea
jungsuek@snu.ac.kr

***Abstract*—We propose an end-to-end DC-to-DC efficiency maximization framework for array antenna RF-based wireless power transfer (WPT) that jointly accounts for transmit power amplifier (PA) and receive rectifier nonlinearities. While prior studies have mainly addressed PA and rectifier nonlinearities through waveform design, this work focuses on optimizing the practical CW excitation vector under measured device operating constraints, offering a practical framework for RF engineers to design WPT systems and determine the optimal transmit excitation for maximum end-to-end DC power delivery. Using measurement-based piecewise-linear (PWL) models for both PA and rectifier characteristics, we maximize the sum of rectified DC power at the receiver array under a transmit-side DC power budget. By applying semidefinite lifting, the resulting problem admits an efficient semidefinite relaxation (SDR) that provides a tight upper bound and a high-quality feasible solution via rank-one recovery and local refinement. Simulation results show that the proposed method outperforms conventional RF-to-RF efficiency by achieving 38.3% higher received DC power, with a relaxation-to-feasible gap of 1.69%. Experimental validation confirms the accuracy of the proposed framework with less than 8% error.**

***Index Terms*—DC-to-DC Efficiency, Microwave Power Transmission (WPT), Power Transfer Efficiency (PTE), Transmission-Conversion Efficiency (TCE), Wireless Power Transfer (WPT).**

I. Introduction

WIRELESS power transfer (WPT) technology has been rapidly growing along with the explosive growth of electronic devices. Inductive WPT has already been successfully commercialized in mobile devices under the Qi standard [1]. Resonant WPT is also being commercialized through implementation in electric vehicles (EVs) [2]. RF-based WPT, which was the ultimate goal of Nikola Tesla, can transmit power wirelessly over the longest distances among the three methods [3].

However, compared with inductive and resonant WPT, RF-based WPT (hereafter referred to simply as WPT) suffers from low efficiency. Long transmission distances fundamentally reduce propagation efficiency in free space, and the power amplifier (PA) and rectifier introduce additional losses in the circuit domain. This remains one of the major bottlenecks for WPT commercialization.

Numerous studies have investigated WPT efficiency in the RF domain. RF-to-RF efficiency, commonly referred to as power transfer efficiency (PTE), has been optimized through various methodologies [4], [5], [6], [7], [8], [9], [10], [11]. PTE has served as a major figure of merit (FoM) for characterizing WPT system performance. However, PTE alone cannot fully capture the behavior of the entire WPT system, as it neglects the DC-domain introduced by the PA and rectifier.

To address this limitation, several studies have explored combining PTE with rectifier power conversion efficiency (PCE) through joint optimization of beamforming and rectification. Wan *et al.* first introduced the term "transmission-conversion efficiency (TCE)," defined as the product of PTE and PCE [12]. Subsequently, Shen *et al.* [13] and Ma *et al.* [14] investigated TCE optimization via beamforming control for the linear and saturation regions of the rectifier, respectively. However, these approaches rely on idealized mathematical models that may not fully capture practical rectifier behavior, and more importantly, they still do not account for PA nonlinearities.

Since practical WPT systems consume DC power at the transmitter and deliver DC power to the load at the receiver,

DC-to-DC efficiency represents the most comprehensive end-to-end FoM for WPT systems. Recent studies have addressed end-to-end efficiency through joint waveform design that accounts for PA and energy harvester nonlinearities [15], [16]. However, these approaches focus on multi-tone waveform optimization and assume behavioral rectifier models limited to the linear operating region, without directly providing the array excitation pattern for practical deployment. This paper instead proposes a CW-based DC-to-DC maximization framework with measurement-based PA and rectifier models across their full operating ranges. Compared to multi-tone waveform approaches, the CW-based formulation with measured device characteristics offers a more practical and accurate representation of RF hardware behavior, and provides the optimal transmit excitation vector for maximum received DC power. The resulting DC-to-DC efficiency is compared with conventional PTE optimization approaches. Section II describes the system model. Section III details the proposed optimization framework. Section IV presents simulation and measurement results, and Section V concludes the paper.

II. System Architecture

This section describes the WPT system architecture considered in this work. Fig. 1 illustrates the system configuration. The transmitter array (TXA) consists of M elements, each with individually controllable magnitude and phase. The receiver array (RXA) includes N rectifiers and a combining circuit, where ideal DC power combining is assumed.[1]

The first stage represents the PA, where the DC-to-RF conversion efficiency is considered. The relationship between the consumed DC power and the output RF power is characterized through measurement. The second stage represents the wireless channel, where the electromagnetic wave propagates through free space. The third stage represents the rectifier, which converts the received RF power to DC with a certain conversion efficiency. The DC outputs from all rectifiers are ideally summed. Based on the figure, our objective is to optimize η_{DC-DC}, which can be expressed as:

$$\eta_{DC-DC} = \eta_{DC-RF} \times \eta_{RF-RF} \times \eta_{RF-DC} \tag{1}$$

III. Proposed Optimization Framework

A. RF-to-RF Efficiency Optimization

Consider the MIMO WPT system shown in Fig. 1. Let $\mathbf{G} \in \mathbb{C}^{N\times M}$ denote the channel matrix between the TXA and RXA, and let $\mathbf{x}_t \in \mathbb{C}^{M\times 1}$ denote the transmit excitation vector. The PTE optimization problem can be formulated as follows [17]:

$$\begin{aligned} \max_{\mathbf{S}} \quad & Q_{RF} := \mathrm{tr}(\mathbf{G}\mathbf{S}\mathbf{G}^H)/Z \\ \text{subject to} \quad & \mathrm{tr}(\mathbf{S})/Z = P_t^{RF}, \quad \mathbf{S} \succeq 0 \end{aligned} \tag{2}$$

where $\mathbf{S} = \mathbb{E}[\mathbf{x}_t\mathbf{x}_t^H]$ is the transmit covariance matrix, Z is the characteristic impedance, and P_t^{RF} is the total transmit RF power constraint. By introducing $\mathbf{S}$, the objective function becomes linear in the optimization variable, enabling efficient convex optimization.[2] Since Q_{RF} represents the total received RF power across the N receivers, maximizing Q_{RF} under a fixed transmit power P_t^{RF} is equivalent to maximizing the PTE. This convex problem guarantees a globally optimal solution $\mathbf{S}^*$. The optimal transmit vector $\mathbf{x}_t^*$ can then be obtained via eigenvalue decomposition of $\mathbf{S}^*$.

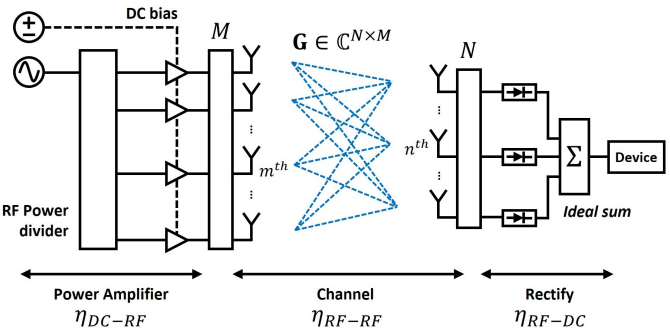

Fig. 1. Block diagram of the MIMO WPT system with three efficiency stages: PA (η_{DC-RF}), channel (η_{RF-RF}), and rectifier (η_{RF-DC}).

B. DC-to-DC Efficiency Optimization via SDR

Building upon the RF-to-RF optimization formulation, we now incorporate the PA and rectifier nonlinearities. Let $p_{\mathrm{TX},m}(\mathbf{S}) = S_{mm}/Z$ denote the transmit RF power at the m-th antenna, and let $p_{\mathrm{RX},i}(\mathbf{S}) = \mathrm{tr}(\mathbf{C}_i\mathbf{S})/Z$ denote the received RF power at the i-th rectifier, where $\mathbf{C}_i = \mathbf{G}^H\mathbf{E}_i\mathbf{G}$ and $\mathbf{E}_i \in \mathbb{R}^{N\times N}$ is a selection matrix for the i-th receiver.

The PA and rectifier characteristics are modeled using measurement-based PWL functions. The rectifier DC output is represented by a concave PWL function $f(p) = \min_{k\in\mathcal{K}}(a_k p + b_k)$, while the PA DC consumption is represented by a convex PWL function $h(p) = \max_{\ell\in\mathcal{L}}(\alpha_\ell p + \beta_\ell)$. We assume that all PAs and rectifiers have identical characteristics and operating ranges.

By introducing auxiliary variables t_i (DC output of the i-th rectifier) and u_m (DC consumption of the m-th PA), the DC-to-DC optimization problem can be formulated as follows:

$$\begin{aligned} \max_{\mathbf{S},\mathbf{t},\mathbf{u}} \quad & \sum_{i=1}^{N} t_i \\ \text{subject to} \quad & \sum_{m=1}^{M} u_m \le P_t^{DC} \\ & \mathbf{S} \succeq 0 \\ & t_i \le a_k\, p_{\mathrm{RX},i}(\mathbf{S}) + b_k, \quad \forall i, \forall k \in \mathcal{K} \\ & p_{\mathrm{RX},i}^{\min} \le p_{\mathrm{RX},i}(\mathbf{S}) \le p_{\mathrm{RX},i}^{\max}, \quad \forall i \\ & u_m \ge \alpha_\ell\, p_{\mathrm{TX},m}(\mathbf{S}) + \beta_\ell, \quad \forall m, \forall \ell \in \mathcal{L} \\ & p_{\mathrm{TX},m}^{\min} \le p_{\mathrm{TX},m}(\mathbf{S}) \le p_{\mathrm{TX},m}^{\max}, \quad \forall m \end{aligned} \tag{3}$$

[1] Realistic, non-ideal DC combining modeling and formulation of multiple rectifiers is beyond the scope of this work.

[2] As a trade-off, the solution $\mathbf{S}^*$ may have rank greater than one; this issue is addressed in Section III-C.

Algorithm 1 Rank-One Recovery and Local Refinement

Require: SDP solution $\mathbf{S}^*$, eigenvectors to combine K
Ensure: Feasible transmit vector $\mathbf{x}_t^*$
Step 1: Eigenvector Extraction & Scaling
Compute EVD: $\mathbf{S}^* = \sum_i \lambda_i \mathbf{v}_i \mathbf{v}_i^H$
Extract $\mathbf{x}_{\text{evd}} = \sqrt{\lambda_1}\mathbf{v}_1$
Find γ via bisection for feasibility
$\mathbf{x}_{\text{scaled}} \leftarrow \gamma \cdot \mathbf{x}_{\text{evd}} / \|\mathbf{x}_{\text{evd}}\|$
Step 2: Eigenvector Combination Search
for each $(c_1, c_2, \ldots, c_K)$ in grid **do**
    $\mathbf{x} \leftarrow \sum_{i=1}^{K} c_i \mathbf{v}_i$
    Scale $\mathbf{x}$ to feasibility, evaluate objective
end for
Save top candidates $\{\mathbf{x}^{(j)}\}$
Step 3: Multi-Start Local Refinement
for each starting point $\mathbf{x}^{(j)}$ **do**
    repeat
        Update via gradient ascent or random perturbation
        Scale to feasibility, accept if objective improves
    until convergence
end for
return $\mathbf{x}_t^* = \arg\max_{\mathbf{x}} \sum_i f(p_{\text{RX},i}(\mathbf{x}))$

The objective maximizes the total rectified DC power at the RXA, subject to a transmit-side DC power budget P_t^{DC}. Note that unlike the RF-to-RF formulation where the transmit RF power is fixed at P_t^{RF} (equality constraint), the DC-to-DC formulation constrains the total DC consumption to be at most P_t^{DC} (inequality constraint), providing additional flexibility in the optimization.[3] The rectifier behavior is captured by the hypograph constraints on t_i, with valid input power ranges enforced for each rectifier. Similarly, the PA DC consumption is modeled via epigraph constraints on u_m, with operating range limits for each PA. Since all constraints are linear in $\mathbf{S}$, $\mathbf{t}$, and $\mathbf{u}$, this formulation is a semidefinite program (SDP) that can be efficiently solved using standard convex optimization tools. The optimal solution $\mathbf{S}^*$ provides a global optimized result for DC-to-DC efficiency.

C. Rank-One Recovery and Local Refinement

Although the SDP in (3) is convex and can be solved globally, the optimal solution $\mathbf{S}^*$ may have rank greater than one due to the relaxation. In such cases, a feasible transmit vector $\mathbf{x}_t^*$ must be extracted from $\mathbf{S}^*$. We propose a three-step procedure to obtain a high-quality rank-one solution.

Step 1: Eigenvector Extraction and Feasibility Scaling. Perform eigenvalue decomposition on $\mathbf{S}^* = \sum_i \lambda_i \mathbf{v}_i \mathbf{v}_i^H$, where $\lambda_1 \geq \lambda_2 \geq \cdots$. The dominant eigenvector $\mathbf{x}_{\text{evd}} = \sqrt{\lambda_1}\mathbf{v}_1$ is extracted as an initial candidate.[4] Since $\mathbf{x}_{\text{evd}}$ may violate the PA or rectifier constraints, we apply uniform scaling $\mathbf{x} = \gamma \mathbf{x}_{\text{evd}} / \|\mathbf{x}_{\text{evd}}\|$ and find the optimal γ via bisection to maximize the objective while satisfying all constraints.

Step 2: Eigenvector Combination Search. When $\mathbf{S}^*$ has multiple significant eigenvalues, *combining all eigenvectors* yields better solutions than using $\mathbf{v}_1$ alone. We form candidate solutions as $\mathbf{x} = \sum_{i=1}^{K} c_i \mathbf{v}_i$ with complex coefficients c_i, and perform a grid search over the magnitude and phase of each coefficient. The top candidates are retained and saved.

Step 3: Multi-Start Local Refinement. Starting from the best candidates obtained in Step 2, we apply local refinement using a combination of numerical gradient ascent and random perturbation. Multiple starting points are used to avoid convergence to poor local optima. The solution with the highest objective value across all runs is selected as the final vector $\mathbf{x}_t^*$.

This procedure bridges the gap between the SDP upper bound (efficiency provided by $\mathbf{S}^*$, which is not directly usable in a real transmitter) and a feasible rank-one solution $\mathbf{x}_t^*$ (the actual transmit excitation vector) for practical implementation. The whole process is well organized in Algorithm 1.

[3]This relaxation is necessary due to the tight operating ranges.

[4]In rank-one $\mathbf{S}^*$ cases such as RF-to-RF efficiency optimization, this dominant eigenvector simply becomes $\mathbf{x}_t^*$ which is also unique.

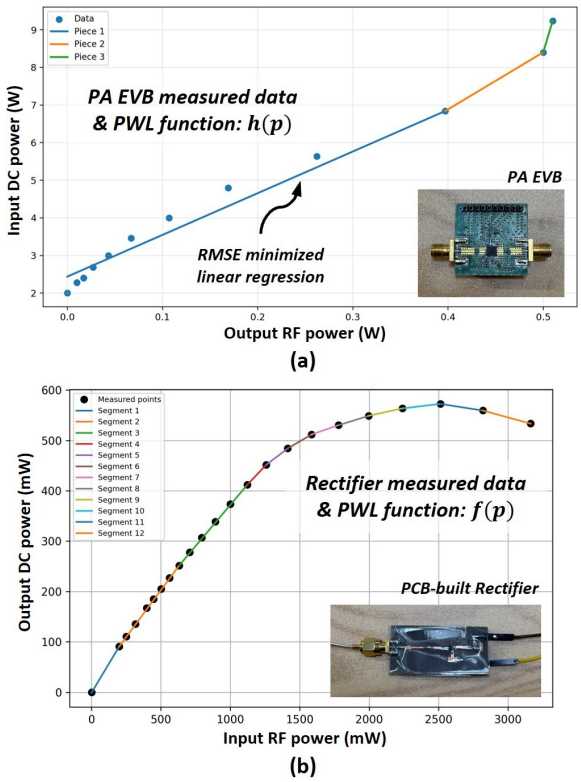

Fig. 2. Measured data and PWL fitting: (a) PA DC consumption versus RF output power and (b) rectifier DC output power versus RF input power.

IV. Results

A. Simulation Setup

The simulation considers a MIMO WPT system with a 16×16 TXA and a 5×5 RXA operating at 5.64 GHz. The TXA consists of 256 linearly polarized (LP) patch antenna elements with 0.6λ spacing. The channel matrix $\mathbf{G}$ is computed assuming free-space propagation with active element patterns. Since the optimization framework depends only on $\mathbf{G}$, it readily generalizes to arbitrary array sizes and TXA-RXA

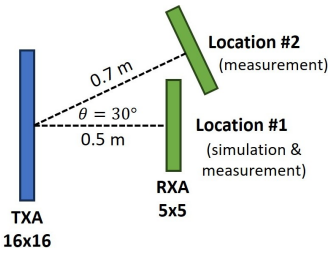

Fig. 3. Simulation and measurement scenarios. RF-to-RF versus DC-to-DC optimization is compared at 0.5 m face-to-face. Simulation-measurement validation is performed at 0.5 m (0°) and 0.7 m (30° offset).

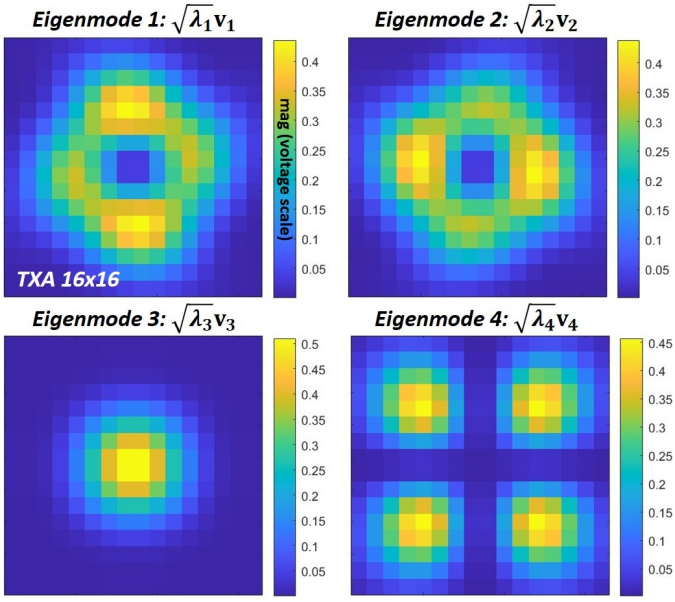

Fig. 4. Magnitude distribution of the four eigenmodes of $\mathbf{S}^*$ over the 16×16 TXA. The SDP solution has rank 4, requiring the rank-one recovery procedure.

configurations. All simulations are performed in MATLAB on an AMD Ryzen 7 5800X processor.

The PA characteristics are obtained from measurements of the Skyworks SE5004L-EK1 evaluation board (EVB), which uses the same PA integrated circuit as the TXA prototype. The DC consumption versus RF output power is measured and fitted to a convex PWL function $h(p)$. The rectifier is a custom-designed half-wave rectifier using the HSMS-2860 Schottky diode with a 370 Ω load. The RF-to-DC conversion characteristic is measured by sweeping the input RF power using a signal generator and recording the output DC current, which is then converted to DC power and fitted to a concave PWL function $f(p)$. Fig. 2 shows the fabricated devices and their measured characteristics, respectively.

For simulation, a face-to-face scenario at 0.5 m distance is considered to compare RF-to-RF and DC-to-DC optimization.[5] For measurement validation, both 0° and 30° angular misalignment scenarios are tested, as illustrated in Fig. 3. The transmit-side DC power budget is set to $P_t^{DC} = 1000$ W.[6]

TABLE I
POWER COMPARISON BETWEEN RF-RF AND DC-DC OPTIMIZATION

Parameter	RF-RF Opt.	DC-DC Opt.
TX DC consumption	989 W	1000 W
TX RF output (Ref.)	33.89 W	33.89 W
RX RF input	26.51 W	24.05 W
RX DC output	6.32 W	8.74 W

TABLE II
EFFICIENCY COMPARISON BETWEEN RF-RF AND DC-DC OPTIMIZATION

Metric	RF-RF Opt.	DC-DC Opt.
RF-to-RF efficiency (η_{RF-RF})	78.22%	70.97%
DC-to-DC efficiency (η_{DC-DC})	0.64%	0.87%

B. Simulation Results

The SDP in (3) is solved for the face-to-face scenario (0.5 m, 0°), and the resulting optimal solution $\mathbf{S}^*$ has rank 4. The entire optimization process completes in under 15 minutes.[7] Fig. 4 shows the magnitude distribution of the four eigenvectors $\mathbf{v}_1$ through $\mathbf{v}_4$ over the 16×16 TXA. Each eigenvector exhibits a distinct spatial pattern: modes 1 and 2 show vertically separated distributions, mode 3 concentrates power at the array center, and mode 4 forms four separate clusters near the corners. Since $\mathbf{S}^*$ is not rank-one, the rank-one recovery procedure described in Section III-C is applied to obtain the final transmit vector $\mathbf{x}_t^*$.

Table I summarizes the power flow for both optimization methods in the face-to-face scenario (0.5 m, 0°). To ensure a fair comparison, the transmit RF power constraint for RF-to-RF optimization is set equal to the TXA RF output obtained from DC-to-DC optimization (33.89 W).[8]

The RF-to-RF optimization achieves higher received RF power (26.51 W) compared to DC-to-DC optimization (24.05 W), as expected from its objective function. However, the received DC power clearly shows the expected result: DC-to-DC optimization yields 8.74 W, which is 38.3% higher than the 6.32 W achieved by RF-to-RF optimization. This improvement is attributed to the joint consideration of PA and rectifier nonlinearities in the proposed formulation. Table II compares the efficiency metrics. While RF-to-RF optimization achieves a higher RF-to-RF efficiency (78.22% vs. 70.97%), the proposed

[5]Ideally, comparing all three optimization approaches (RF-to-RF, RF-to-DC, and DC-to-DC) would be more comprehensive. However, this is beyond the scope of this paper; RF-to-RF serves as a reasonable baseline due to its widespread use as a standard FoM.

[6]In the future extended paper, we will discuss the effects of varying P_t^{DC}.

[7]The proposed algorithm is intended for offline system design rather than real-time control; hence, computation time is not critical. Furthermore, MATLAB's default CPU-based execution is not optimized for speed.

[8]This is necessary because DC-to-DC optimization is already constrained by the DC power budget of 1000 W, not by the RF output power.

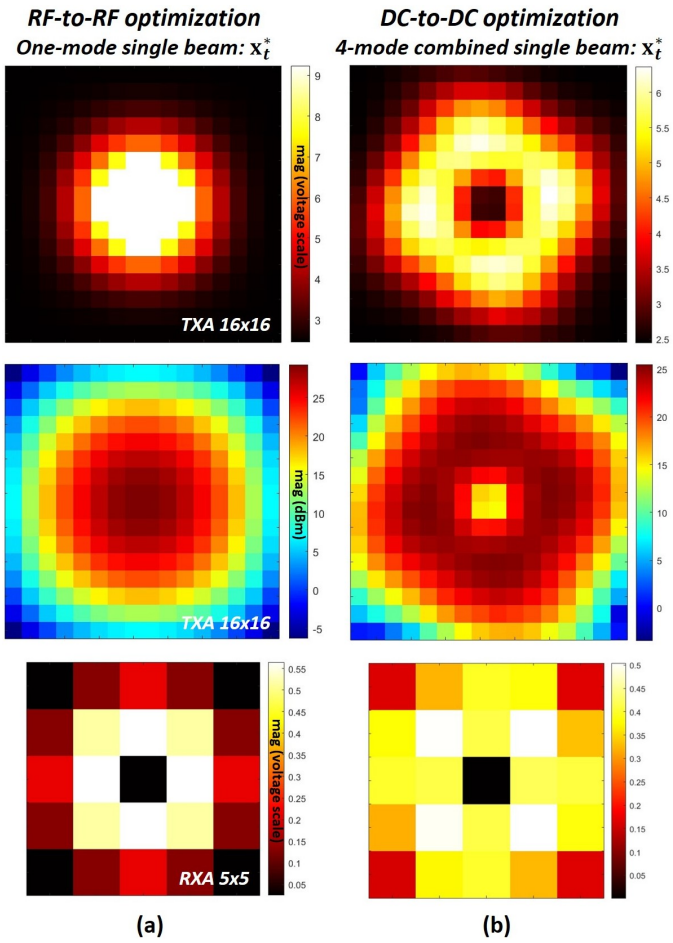

Fig. 5. Power distribution comparison between (a) RF-to-RF and (b) DC-to-DC optimization. Top row: PA DC consumption at the 16×16 TXA. Middle row: TX RF output power. Bottom row: received DC power at the 5×5 RXA.

DC-to-DC optimization achieves a 36.0% improvement in end-to-end DC-to-DC efficiency (0.87% vs. 0.64%).[9] The *SDP relaxation-to-feasible gap*, defined as the difference between the SDP upper bound (ideal optimal, calculated by $\mathbf{S}^*$) and the final rank-one solution (true excitation vector, TXA excited by $\mathbf{x}_t^*$), is only 1.69%, indicating that the proposed rank-one recovery procedure effectively extracts a near-optimal solution.

Fig. 5 illustrates the power distribution at the TXA and RXA for both optimization methods. The top row shows the PA DC consumption, the middle row shows the TX RF output power, and the bottom row shows the received DC power at the RXA. In the RF-to-RF case (a), the optimizer concentrates RF power at the center of the RXA, causing the center rectifiers to exceed their optimal input range and resulting in reduced DC output. Meanwhile, the outer rectifiers receive low power, also yielding poor DC output. In contrast, the DC-to-DC case (b) more broadly distributes power to maximize the DC output through the rectifier arrays, resulting in a more uniform and higher overall DC power.

[9]The absolute DC-to-DC efficiency is limited by the use of commercial PAs and a simple half-wave rectifier; higher efficiency can be achieved with optimized components. The focus of this work is the optimization framework itself, which enables system-level DC-to-DC efficiency evaluation.

Fig. 6. Hardware setup for DC-to-DC optimization validation.

TABLE III
COMPARISON OF SIMULATED AND MEASURED RECEIVED DC POWER

Scenario	Simul.	Meas.	Error
0° (0.5 m)	8.74 W	8.27 W	5.4%
30° (0.7 m)	7.60 W	7.02 W	7.6%

C. Measurement Results

To validate the proposed optimization framework, measurements are conducted for two scenarios: 0.5 m face-to-face (0°) and 0.7 m with 30° angular offset (as shown in Fig. 3). Fig. 6 shows the measurement setup [18], [19], [20], [21]. Since ideal DC power combining is assumed in the formulation, each rectifier's DC output power is measured independently and summed to obtain the total power.[10]

Table III compares the simulated and measured received DC power for the DC-to-DC optimized excitation vector. The measured results show good agreement with the simulation, with errors of 5.4% and 7.6% for the 0° and 30° scenarios, respectively. These discrepancies can be attributed to fabrication tolerances, channel estimation errors, and non-ideal rectifier behavior. The results demonstrate that the proposed algorithm can be accurately applied to practical WPT systems.

V. CONCLUSION AND FUTURE EXTENSIONS

This paper proposes an end-to-end DC-to-DC efficiency maximization framework for WPT systems that incorporates measured PA and rectifier characteristics across their full operating ranges, offering a practical and accurate approach for determining the optimal transmit excitation vector. Using measurement-based PWL models, the optimization problem is formulated as a semidefinite program, which provides a global upper bound. A three-step rank-one recovery procedure is developed to extract a feasible transmit excitation vector from the high-rank SDP solution. Simulation results demonstrate

[10]Practical DC combining circuit design is beyond the scope of this work.

that the proposed DC-to-DC optimization achieves 38.3% higher received DC power compared to conventional RF-to-RF optimization, with only a 1.69% relaxation-to-feasible gap. Measurement validation shows good agreement with simulations, with errors of 5.4% and 7.6% for the 0° and 30° scenarios, respectively.

Future work will provide a comprehensive comparison among RF-to-RF, RF-to-DC [22], and DC-to-DC optimization approaches, along with extended analysis on various system parameters.

Acknowledgment

This work was supported by Institute of Information & Communications Technology Planning & Evaluation (IITP) grant funded by the Korea government (MSIT) (No. 2019-II190098, Advanced and integrated software development for electromagnetic analysis).

References

[1] M. Budhia, G. Covic, and J. Boys, "A new IPT magnetic coupler for electric vehicle charging systems," in *Proc. 36th Annu. Conf. IEEE Ind. Electron. Soc. (IECON)*, 2010, pp. 2487–2492, doi: 10.1109/IECON.2010.5675350.

[2] A. Kurs, A. Karalis, R. Moffatt, J. D. Joannopoulos, P. Fisher, and M. Soljačić, "Wireless power transfer via strongly coupled magnetic resonances," *Science*, vol. 317, no. 5834, pp. 83–86, 2007, doi: 10.1126/science.1143254.

[3] W. Brown, "The technology and application of free-space power transmission by microwave beam," *Proc. IEEE*, vol. 62, no. 1, pp. 11–25, 1974, doi: 10.1109/PROC.1974.9380.

[4] G. Oliveri, L. Poli, and A. Massa, "Maximum efficiency beam synthesis of radiating planar arrays for wireless power transmission," *IEEE Trans. Antennas Propag.*, vol. 61, no. 5, pp. 2490–2499, 2013, doi: 10.1109/TAP.2013.2241714.

[5] S. Kojima, T. Mitani, and N. Shinohara, "Array optimization for maximum beam collection efficiency to an arbitrary receiving plane in the near field," *IEEE Open J. Antennas Propag.*, vol. 2, pp. 95–103, 2021, doi: 10.1109/OJAP.2020.3044443.

[6] H. Y. Kim, Y.-S. Lee, and S. Nam, "Efficiency bound estimation for a practical microwave and mmwave wireless power transfer system design," *J. Electromagn. Eng. Sci.*, vol. 23, no. 1, pp. 69–74, 2023, doi: 10.26866/jees.2023.1.r.146.

[7] X. Yang, W. Geyi, and H. Sun, "Optimum design of wireless power transmission system using microstrip patch antenna arrays," *IEEE Antennas Wireless Propag. Lett.*, vol. 16, pp. 1824–1827, 2017, doi: 10.1109/LAWP.2017.2682262.

[8] Y.-S. Lee, J. Oh, and S. Nam, "An effect of time reversal based multiple beacon selection on wireless power transfer performance," in *Proc. 2024 Int. Symp. Antennas and Propag. (ISAP 2024)*, Incheon, Republic of Korea, Nov. 2024, pp. 1–2, doi: 10.1109/ISAP62502.2024.10846697.

[9] A. Hajimiri, B. Abiri, F. Bohn, M. Gal-Katziri, and M. H. Manohara, "Dynamic focusing of large arrays for wireless power transfer and beyond," *IEEE J. Solid-State Circuits*, vol. 56, no. 7, pp. 2077–2101, 2021, doi: 10.1109/JSSC.2020.3036895.

[10] Y.-S. Lee, J. Oh, and S. Nam, "Sequential feedback-based phase optimization using hadamard basis for wireless power transfer," in *Proc. 2025 IEEE Wireless Power Technol. Conf. Expo (WPTCE 2025)*, Rome, Italy, Jun. 2025, pp. 1–5, doi: 10.1109/WPTCE62521.2025.11062191.

[11] T. Yoon *et al.*, "Overcoming efficiency degradation in wireless power transfer systems: A supply voltage modulation method empowered by 5.64-GHz 256-element antenna array receiving 10.6-Watt," in *Proc. 2025 IEEE MTT-S Int. Microw. Symp. (IMS 2025)*, San Francisco, CA, USA, Jun. 2025, pp. 85–88, doi: 10.1109/IMS40360.2025.11104047.

[12] S. Wan and K. Huang, "Methods for improving the transmission-conversion efficiency from transmitting antenna to rectenna array in microwave power transmission," *IEEE Antennas Wireless Propag. Lett.*, vol. 17, no. 4, pp. 538–542, 2018, doi: 10.1109/LAWP.2018.2801320.

[13] S. Shen and B. Clerckx, "Beamforming optimization for mimo wireless power transfer with nonlinear energy harvesting: rf combining versus dc combining," *IEEE Trans. Wireless Commun.*, vol. 20, no. 1, pp. 199–213, 2021, doi: 10.1109/TWC.2020.3024064.

[14] G. Ma, J. Xu, Y. Zeng, and M. R. V. Moghadam, "A generic receiver architecture for MIMO wireless power transfer with nonlinear energy harvesting," *IEEE Signal Process. Lett.*, vol. 26, no. 2, pp. 312–316, 2019, doi: 10.1109/LSP.2018.2890164.

[15] J. Zhang and B. Clerckx, "Waveform design for wireless power transfer with power amplifier and energy harvester non-linearities," *IEEE Trans. Signal Process.*, vol. 71, pp. 2638–2653, 2023, doi: 10.1109/TSP.2023.3278374.

[16] A. B. Khattak, O. L. A. López, A. Azarbahram, D. Kumar, and M. Latva-Aho, "End-to-end waveform and beamforming optimization for rf wireless power transfer," in *2024 IEEE 25th International Workshop on Signal Processing Advances in Wireless Communications (SPAWC)*, 2024, pp. 516–520, doi: 10.1109/SPAWC60668.2024.10694404.

[17] Y.-S. Lee, J. Oh, and S. Nam, "Effects of magnitude dynamic range constraints on MIMO wireless power transfer efficiency," in *Proc. 2025 Int. Symp. Antennas and Propag. (ISAP 2025)*, Fukuoka, Japan, Oct. 2025, pp. 1–2, doi: 10.23919/ISAP63122.2025.11361879.

[18] Y.-S. Lee *et al.*, "LUT-based transmit mode calibration complexity reduction method for wireless power transfer," in *Proc. 2024 IEEE Wireless Power Technol. Conf. Expo (WPTCE 2024)*, Kyoto, Japan, May 2024, pp. 137–141, doi: 10.1109/WPTCE59894.2024.10557392.

[19] Y.-S. Lee *et al.*, "A design and characterization method of a scalable large transmitting array for wireless power transfer," *IEEE Trans. Microw. Theory Techn.*, vol. 73, no. 6, pp. 3346–3358, 2025, doi: 10.1109/TMTT.2024.3487911.

[20] Y.-S. Lee, T. Yoon, J. Oh, and S. Nam, "Design and calibration of a CW time reversal wireless power transfer transmitter with pilot signal detection *(Invited Paper)*," in *Proc. 2025 Asia-Pacific Microw. Conf. (APMC 2025)*, Jeju, Republic of Korea, Dec. 2025, pp. 1–3, doi: 10.1109/APMC65046.2025.11378159.

[21] T. Yoon, U. Park, M. Kim, S. Lee, Y.-S. Lee, S. Nam, and J. Oh, "A topology-based array compensation empowered by equivalent current modeling of tm10 patch antennas for cross-polarization reduction," *IEEE Open J. Antennas Propag.*, vol. 6, no. 6, pp. 1696–1707, 2025, doi: 10.1109/OJAP.2025.3592198.

[22] Y.-S. Lee, T. Yoon, Y. J. Song, S. K. Hong, J. Oh, and S. Nam, "Transmission-conversion efficiency maximization technique for MIMO wireless power transfer systems in ISAC applications," *IEEE Antennas Wireless Propag. Lett.*, vol. 24, no. 11, pp. 4492–4496, 2025, doi: 10.1109/LAWP.2025.3578089.